

## Electronic structure and stability of ring clusters in the Si(111)-( $\sqrt{7}\times\sqrt{7}$ )Co surface

Min-Hsiung Tsai, John D. Dow, and Peter A. Bennett

*Department of Physics and Astronomy, Arizona State University, Tempe, Arizona 85287-1504*

David G. Cahill

*Department of Materials Science and Engineering, University of Illinois at Urbana-Champaign, Urbana, Illinois 61801*

(Received 11 January 1993)

The ring-cluster structure of the Si(111)-( $\sqrt{7}\times\sqrt{7}$ )Co surface is investigated by comparing local-density approximation, spin-dependent pseudofunction theoretical results with data. In the ring-cluster model, each surface unit cell contains a single Co atom substituting for a Si surface atom; this Co atom is then covered by three "bridging" and three "capping" Si adatoms, yielding  $C_3$  point-group symmetry with respect to the Co site. We confirm the energetic stability of the ring-cluster structure, and determine atomic coordinates, including the height, 0.46 Å, that the Co atom lies *above* the surface plane. Scanning-tunneling-microscopy (STM) images are calculated from the energy-selected electronic-charge densities, and show the threefold (Si capping adatoms) and onefold (Co atoms) structures in the surface unit cell that are experimentally observed for empty and filled states, respectively. The surface density of states is computed to be that of an insulator, in agreement with the tunneling spectra. The predicted surface magnetic moments are small, and the surface electronic structure is calculated for future comparison with photoemission measurements. The relatively small computed barrier height of  $\approx 0.4$  eV per adatom pair between the two degenerate orientations of an isolated cluster suggests that the cluster geometry may switch relatively rapidly at room temperature between the two orientations, giving rise to the toroidal  $C_6$ -symmetric appearance of isolated clusters in STM images.

### I. INTRODUCTION

The atomic geometries of transition-metal/silicon (TM/Si) structures at surfaces and interfaces must be determined for both practical and fundamental reasons. On the practical side, transition-metal silicides metallize Si at high temperatures, and also provide rectifying junctions with a variety of Schottky barrier heights.<sup>1,2</sup> On the fundamental side, several transition-metal silicides grow epitaxially as single-crystal overlayers, and are prototypes of both metal-silicon interfaces and metallization for a variety of other semiconductors. The unfilled  $d$  shells of the Co atoms at these interfaces complicate theoretical studies, and cause computations of the surface electronic properties to be especially challenging.<sup>3</sup> But the most difficult theoretical challenge, by far, lies in the determination of the equilibrium surface geometrical structure.

The observation that most transition-metal silicides display strongly exothermic reactions with Si, forming a variety of silicides with a propensity for epitaxy,<sup>4</sup> suggests that TM/Si surface reconstructions will likely involve extensive rearrangements of surface atoms, rather than simple decoration of the pristine silicon surface. Several periodic or superlattice surface reconstructions have been observed in TM/Si(111) systems,<sup>5-7</sup> although the atomic structures of these surfaces remain largely unknown and unexplored. One notable exception is the Si(111)-( $\sqrt{7}\times\sqrt{7}$ )Co surface formed by one-seventh of a monolayer of Co on the Si(111) surface, for which a ring-cluster model has been proposed.<sup>8</sup> Since the bonding in the ring-cluster model is quite unusual, theoretical inves-

tigation of its structure, and determination of whether or not the proposed model corresponds to a minimum free-energy state of the surface is warranted.

In this paper, we explore the electronic properties and energetic stability of the ring-cluster model, using the spin-dependent pseudofunction scheme for executing computations in the local-spin-density approximation. We compute the free energy at zero temperature (namely the total internal energy) for the surface in various configurations, and determine the minimum-energy configuration. We confirm the energetic stability of the proposed ring-cluster model, compute equilibrium atomic coordinates, and predict the surface electronic structure of the model for future comparison with photoemission data.

### II. RING-CLUSTER MODEL

The ring-cluster model<sup>8</sup> of the  $\sqrt{7}\times\sqrt{7}$  surface was deduced from scanning-tunneling-microscopy (STM) images and medium-energy ion-scattering measurements (with channeling and blocking) for one-seventh monolayer of Co on a Si(111) surface which was annealed at 670°C. It features a hexagonal  $\sqrt{7}\times\sqrt{7}R19.1^\circ$  structure (Figs. 1 and 2). That is, the  $\sqrt{7}\times\sqrt{7}$  surface unit is rotated 19.1° with respect to the hexagonal unit cell of the pristine surface. In this model, Co atoms substitute for Si atoms at the (111) surface, and are then each covered by a ring cluster of six Si atoms; the Co atoms and their ring clusters form a periodic hexagonal close-packed array on the surface. The surface unit cell contains a single Co atom (which replaces a Si atom on the surface of the

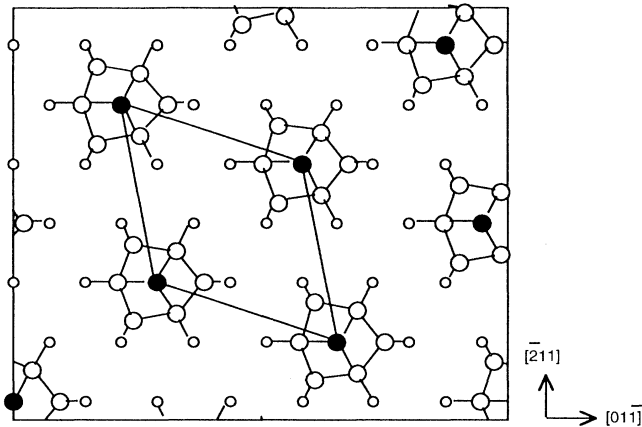


FIG. 1. Top view of the ring-cluster model of the Si(111)- $(\sqrt{7}\times\sqrt{7})$ Co surface. One  $\sqrt{7}\times\sqrt{7}$  surface unit cell is outlined. It contains a single Co atom (very large filled circles) substitutional for a Si atom in the top substrate layer (substrate Si atoms are denoted by small open circles) and a ring cluster of six Si adatoms (large open circles) located above the Co, with three "bridging Si adatoms" (each bonded to the Co atom, one Si substrate atom, and two capping adatoms), and three "capping adatoms," each bonded to two bridging adatoms and one Si substrate atom. Capping adatoms are slightly farther from the Co than bridging adatoms, and are not directly bonded to the Co. The Co atoms are each bonded to three second-layer Si atoms, giving each Co a coordination of six.

"substrate"), plus the ring cluster of six adatoms located above the Co: three Si "bridging adatoms" and three Si "capping adatoms," as shown in Figs. 1 and 2. The bridging atoms are fourfold coordinated, while the capping atoms are threefold coordinated, with one dangling bond each. The coordinates of the atoms are given in Ref. 9, and may be compared with the coordinates of

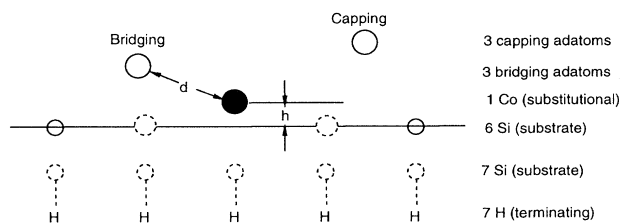


FIG. 2.  $[\bar{2}11]$  projection (side view) of a single unit cell of the ring-cluster model structure used for the calculation. Solid circles lie in the  $(\bar{2}11)$  section plane through the Co atom at the center of the cluster (a horizontal line in Fig. 1). Dotted circles represent the projected positions of some atoms not in the section plane. (We do not show either bridging or capping Si adatoms that are not in the section plane.) The number of each type of atom in the surface unit cell is indicated on the side of the drawing. The horizontal line represents the nominal Si(111) surface (i.e., the top of the substrate bilayer). The Co atom (filled circle) is sixfold coordinated, with three bonds to atoms (the nearest dotted circles) in the second layer of the bilayer substrate, and three bonds to "bridging adatoms" (open solid circles) with bond length  $d$ . The variable parameters of the calculation are  $d$  and  $h$ . The bottom layer consists of H atoms.

CoSi<sub>2</sub>.<sup>10</sup> The point-group symmetry at the Co site is  $C_3$ ,<sup>11</sup> i.e., threefold rotational symmetry. In this model, all dangling Si bonds of the substrate's Si(111) surface are saturated, leaving three dangling bonds (one on each of the capping atoms) per  $\sqrt{7}\times\sqrt{7}$  surface unit cell.

### III. METHOD

#### A. Theory

For calculating the electronic structure, we first need a model of bulk Si (the "substrate") with a pristine, unrelaxed (111) surface. To minimize the time of computation, we use only a bilayer of Si atoms to simulate the bulk substrate, terminating the Si dangling bonds on the bottom layer of this bilayer with H atoms.<sup>12</sup>

The (volume) unit cell for our calculations consists of the surface unit cell discussed above (one Co atom, three bridging Si atoms, and three capping Si atoms) plus 20 Si and H atoms of the substrate: From the bottom up we have a total of 27 atoms in the volume unit cell: (i) seven bottom-layer H atoms terminating the Si dangling bonds of the layer above, with the Si-H bond length taken to be the sum of Si and H covalent radii, 1.43 Å;<sup>13</sup> (ii) seven second-layer substrate Si atoms; (iii) a top layer of the substrate with six Si atoms and one Co atom; (iv) three bridging Si adatoms; and (v) three capping Si adatoms. See Fig. 2.

Our basic theoretical approach is to compute the free energy of the surface at zero temperature, namely the total internal energy, for the surface in various different configurations close to the proposed ring-cluster configuration, and to determine the minimum-energy configuration, thereby providing an energetic justification of the model. Thus we shall show that the ring-cluster model is a *stable* geometric structure of Co on the Si(111) surface. To do this, ideally we would employ the *a priori* self-consistent local-density approximation<sup>14</sup> to find the minimum-energy configuration of the 27 Si and Co atoms in and above the surface, by varying all of their atomic positions. Such a minimization, considering all possible structures, is computationally impractical, and so we optimize only two structural parameters: (i) the height  $h$  of the Co atom above the surface plane (at  $z=0$ ), and (ii) the distance  $d$  between a Co atom and its nearest-neighbor bridging Si adatoms. (See Fig. 2.) All nearest-neighbor Si-Si distances are fixed to be the bulk Si value of 2.352 Å, corresponding to a Si room-temperature lattice constant of 5.431 Å.<sup>15,16</sup> Note that Co is allowed two bond lengths, one for bonds to bridging Si adatoms and another for bonding to substrate Si atoms; the Si capping atoms are not (directly) bonded to Co.

To allow for the possibility that the Co atoms might be in a magnetic state and spin polarized, we employ the spin-unrestricted pseudofunction implementation of the local-spin-density approximation,<sup>17-19</sup> which is especially well suited for treating localized states, such as the Co  $d$  states. This method<sup>18</sup> has a proven track record of successes for many materials,<sup>17,20-25</sup> ranging from predicting the Curie constants,<sup>17</sup> photoemission data,<sup>20</sup> and inverse photoemission spectra<sup>20</sup> of Cd<sub>1-x</sub>Mn<sub>x</sub>Te substi-

tutional crystalline alloys to determining the spins of Cu and O atoms in the high critical temperature superconductor  $\text{La}_2\text{CuO}_4$ .<sup>17,22</sup> In more mundane materials, such as Si (Ref. 26) or CdTe,<sup>20</sup> where spin polarization is unimportant, the method reproduces the widely accepted results of spin-independent local-density theory. It also predicts equilibrium geometries in agreement with *a priori* local-density-approximation molecular dynamics.<sup>27</sup>

When performing integrations over the surface Brillouin zone, we used Cunningham's single special point  $\mathbf{k}_{\parallel}$  for the two-dimensional hexagonal lattice.<sup>28</sup> This special-point wave vector is given in Ref. 29, appropriately scaled and rotated.

### B. Experiment

Scanning-tunneling-spectroscopy data were measured to provide an experimental test of the calculated electronic structure of the  $\sqrt{7}\times\sqrt{7}$  surface. The  $\sqrt{7}\times\sqrt{7}$  surface was prepared as described previously:<sup>8</sup> 0.1 monolayer (ML) of Co was deposited onto a clean Si(111)  $7\times 7$  surface at room temperature and then the sample was annealed at 670 °C for approximately 10 s. The differential conductance  $dI/dV$  was measured by adding a small modulation to the sample bias and using a lock-in amplifier to measure the resulting modulation of the tunneling current. To increase the dynamic range of the experiment, the tip-sample separation  $s$  was decreased by 1.5 Å as the bias voltage approached zero.<sup>30</sup> The raw data have been normalized to constant  $s$  using the experimentally determined function  $I(s)=I(s_0)\times\exp[1.9(s-s_0)/\text{Å}]$ . As is always true in scanning tunneling spectroscopy, changes in the electronic structure of the tip can produce variations in the data,<sup>31</sup> but differences between spectra recorded at separate surface locations using the same tip are reliable.

## IV. RESULTS

### A. Energetics and bonding of the ring-cluster model

Using a nominal value of the bridging-Si-Co bond length suggested from ion-scattering experiments,  $d=2.3$  Å, we minimized the total energy with respect to the Co height above the surface plane,  $h$ . (See Fig. 2.) The total energy as a function of  $h$  is given in Fig. 3, from which we determined an equilibrium height of  $h=0.463$  Å (above the substrate plane), at which the zero-temperature free energy reaches a minimum. Searching for a minimum total energy by varying  $d$  for this value of  $h$  led to  $d=2.313$  Å $\pm 0.01$  Å, so close to the starting value of  $d=2.3$  Å that we did not need to vary  $h$  and iterate.

It is interesting that the Co atom lies *above* the surface plane, with Co bonds to the Si atoms in the ring cluster that are 2.31 Å long, about the same length as the corresponding bulk  $\text{CoSi}_2$  bonds of 2.324 Å. ( $\text{CoSi}_2$  has a  $\text{CaF}_2$  crystal structure with a lattice parameter 1.2% smaller than the lattice constant of Si.) The bond lengths of Co to the substrate come out to be 2.54 Å long, considerably longer than the bonds to the bridging adatoms. Long

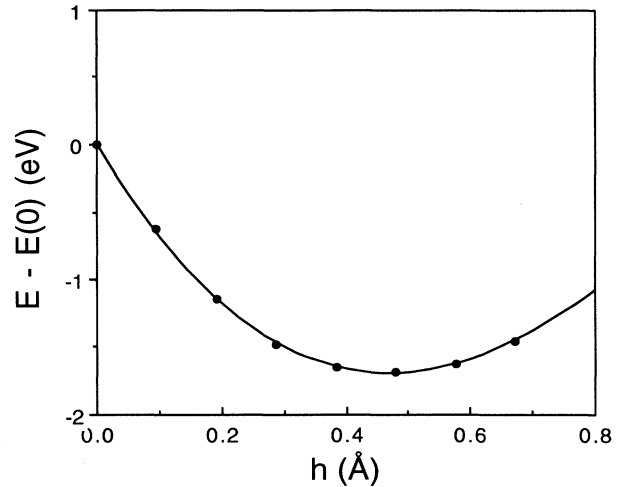


FIG. 3. Calculated total energy per unit cell,  $E$  (in eV), as a function of the height,  $h$ , of the Co adatom above the surface layer, assuming a fixed Co-Si adatom bond length  $d$  of 2.3 Å. The zero of energy is taken to be the value for  $h=0$ .

Co-Si bonds do occur in  $\text{CoSi}$ , which assumes the FeSi crystal type with sevenfold metallic coordination and has three different Co-Si bond lengths in the unit cell: one of 2.28 Å, three of 2.33 Å, and three of 2.47 Å.<sup>32</sup> This longest bond is similar in length to our Co bond with the substrate.

Our value of the height  $h$  of the Co atom above the surface plane is probably the first reliable determination of this difficult-to-measure quantity. We estimate the accuracy of the Co-Si bond lengths determined from these calculations to be  $\pm 0.05$  Å. These bond lengths are more precise than those determined from ion-scattering studies of the ring-cluster structure, since the latter depend on the width of two overlapping blocking dips. We speculate that the rather long Co-Si bonds with the substrate atoms result from the steric constraints on the bridging and capping adatoms, which have well-defined Si-Si spacings but also bond strongly to the Co, and pull it out of the surface.

Double-alignment ion-scattering data directly determine the direction of the Co-Si internuclear axes to be 30.7° and 32.2° with respect to the (111) plane, for the bridging and capping adatoms, respectively.<sup>8</sup> The calculated angle subtended by a Co atom with the  $z=h$  plane [which is parallel to the (111) surface plane] and with a bridging Si adatom is found to be 27.4°; the corresponding angle between that plane and a capping adatom is 30.5°, both close to the measured values.<sup>8</sup>

We have shown that the proposed ring-cluster model's atomic configuration corresponds at least to a *local* minimum of the free energy, and hence is stable with the expected bridging-Si-Co bond length  $d=2.3$  Å, and with the Co lying  $h=0.463$  Å above the surface plane. We also find the angles between Si adatoms and the Si(111) surface plane to be close to the observed angles. These results, taken together, show that the ring-cluster model gives an energetically stable geometry, and that the proposed experimental geometry is almost certainly the

correct one, being virtually identical to the theoretical minimum-energy geometry.

### B. Electronic structure

Once the atomic positions are determined, it is a straightforward if computationally cumbersome matter to compute the surface electronic structure.<sup>33,34</sup> Our results produce rather flat energy bands in the region of energies  $-12 \text{ eV} < E < 0$ , where we have taken the zero of energy at the vacuum level. The Fermi energy is  $E_F = -5.03 \text{ eV}$ , and the work function is  $+5.03 \text{ eV}$ . The energy bands themselves are numerous and show very little dispersion, from which we infer that there is relatively little interaction between clusters. This may explain the observation that the clusters exist independently of their packing, periodic supercrystal structure or long-range order. Figure 4 depicts the calculated density of states projected onto the Co site associated with  $s$ ,  $p$ , and  $d$  orbitals for energies  $-12 \text{ eV} < E < 0$ , and the density of states ( $d$  orbitals only) projected onto the Co site, as well as the density of states projected onto a Si capping site. The density of states from about 3 eV below the Fermi energy  $E_F$  to 1 eV above it is dominated by Co  $d$  orbitals; the  $d$ -band center is about 0.7 eV below  $E_F$ . The flat bands, due primarily to dangling-bond  $p$  orbitals of the Si capping adatoms and  $sp$  orbitals of the Si bridging adatoms, hybridized with the Co  $d$  orbitals, produce the structure

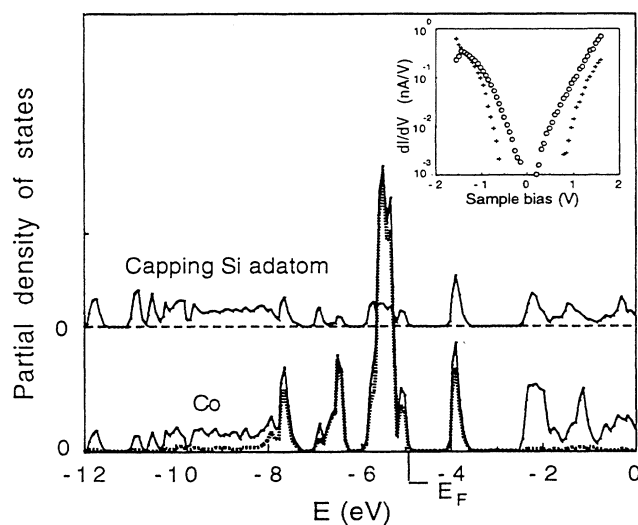


FIG. 4. Densities of states (in arbitrary units) vs energy  $E$  (in eV). The lower panel has states projected onto the Co site, with the dashed line being  $d$  states only. The Fermi energy is indicated at  $-5.03 \text{ eV}$ . The upper panel has states projected onto a capping Si-adatom site. The states about 1 eV above the Fermi energy are mostly due to dangling bonds of the capping Si adatoms, and to the Co  $d$  states, but the capping adatoms are more visible in STM empty-state images because they are closer to the tip. The inset is the STM-measured derivative  $dI/dV$  (in nA/V) vs sample bias  $V$  (in V). The plus signs (circles) are data for the STM tip over the center of a ring cluster (over a surface defect). These data show that there is a gap of more than 1 eV at the surface.

about 1 eV above  $E_F$ . Similar to the case for bulk  $\text{CoSi}_2$ , a quasigap (a real gap for these surface states) in the metal  $d$  bands appears near the Fermi level, and strong  $p$ - $d$  hybridization occurs.<sup>3,35</sup> The peaks near  $-8 \text{ eV}$  are due to the terminating H atoms of the model, and should be disregarded.

The surface layer theoretically has a band gap of 1.0 eV, and so the surface is insulating, in agreement with the experimental tunneling spectra (Fig. 4).

Tunneling spectroscopy data for two locations on the surface are shown in the inset of Fig. 4. Data obtained at the center of a ring cluster show that  $dI/dV$  falls to less than 1% of its initial value in a bias range of  $-0.7 < V_{\text{bias}} < 0.9 \text{ V}$ , clearly demonstrating that the electronic structure of the ring cluster shows a wide separation in energies between filled and empty electronic states. Data obtained at a defect on a boundary between differently oriented  $\sqrt{7} \times \sqrt{7}$  domains are shown as open circles. This defect state does have a significant electronic state density near the Fermi level, and is a likely cause of Fermi-level pinning on the  $\sqrt{7} \times \sqrt{7}$  surface. The microscopic structure of this defect is not known. This measurement also shows that the wide energy gap measured for the  $\sqrt{7} \times \sqrt{7}$  structure is not due to the electronic structure of the tip.

### C. STM images

Experimental STM images of the  $\sqrt{7} \times \sqrt{7}$  surface structure show a number of intriguing features. The images of electronically empty states [Fig. 5(a)] show a trimer structure, with lobes pointing along  $\langle 110 \rangle$  azimuths, the direction of the bond between the Co and the Si capping atoms. (We shall show that these are indeed images of capping Si atoms.) In contrast, the filled states' images [Fig. 5(b)] show a single lobe in each surface unit cell centered on the Co atom. Very high-temperature annealing of the  $\sqrt{7} \times \sqrt{7}$  surface produces a low-density lattice gas of these clusters, with a "perfect  $1 \times 1$ " low-energy

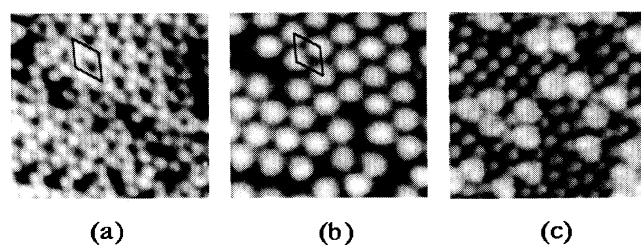


FIG. 5. Experimental STM images showing various arrangements of ring-cluster structures. (a) The empty-state image (bias of  $+2.0 \text{ V}$ ) of the  $\sqrt{7} \times \sqrt{7}$  structure with a single surface unit cell outlined. For close-packed structures, clearly defined trimer lobes point in the directions of the  $\langle 110 \rangle$  azimuths, while isolated clusters take on a more closely sixfold-symmetric appearance. (b) The filled-state image (bias of  $-1.8 \text{ V}$ ) of the matching area showing a single lobe at the center of the trimers. (c) The empty-state image ( $+2.2 \text{ V}$ ) of the (cobalt) "impurity-stabilized  $1 \times 1$ " surface produced by heating to  $1250^\circ \text{C}$ . It is a lattice gas of ring clusters. Again, note the apparent loss of threefold symmetry for individual, isolated ring clusters.

electron-diffraction (LEED) pattern. This is the widely observed “impurity-stabilized” surface [Fig. 5(c)].<sup>8,36</sup> The persistence of the surface unit-cell structures, independent of their packing or long-range order, indicates a remarkable stability of the ring-cluster structure itself. Some clusters on the annealed surface are dispersed and isolated, and exhibit a nearly sixfold symmetry. They look like tiny, well-formed toroids.<sup>8</sup> The apparent sixfold symmetry was attributed to rapid flipping of the cluster between the two degenerate threefold-symmetric ground states of the ring cluster, similar to the flipping between tilted dimers on the Si(100) surface.<sup>37,38</sup>

STM images for the ring-cluster model can be computed using Bardeen’s expression for the tunneling current:<sup>39</sup>

$$I(V) = (2\pi e / \hbar) \sum_{\mu, \nu} f(E_\mu) [1 - f(E_\nu - eV)] \times |M_{\mu, \nu}|^2 \delta(E_\mu - E_\nu), \quad (1)$$

where  $f(E)$  is the Fermi-Dirac function,  $V$  is the bias voltage, and  $M_{\mu, \nu}$  is the transfer-matrix element between the tip state  $\mu$  and the sample state  $\nu$ :

$$M_{\mu, \nu} = -(\hbar^2 / 2m) \int_S d\mathbf{S} (\psi_\mu \nabla \psi_\nu - \psi_\nu \nabla \psi_\mu), \quad (2)$$

where  $\psi_\mu$  and  $\psi_\nu$  are the tip and sample wave functions, respectively, and  $S$  is the surface separating the tip and the sample.

We approximate Bardeen’s formula:

$$I(V) \propto \sum_{\nu} |\psi_\nu(\mathbf{R}_{\text{tip}})|^2 W(E_\nu, E_F, E_F - eV), \quad (3)$$

where the window function  $W(E_\nu, E_F, E_F - eV)$  is unity for  $E_\nu$  between  $E_F$  and  $E_F - eV$ , and zero otherwise. If the window function is replaced by  $-eV\delta(E_\nu - E_F)$ , Eq. (3) reduces to the Tersoff-Hamann formula,<sup>40</sup> which is valid only for small bias voltages  $V$ . The summation on the right-hand side of Eq. (3) is basically an energy-selected sample charge density at the tip position,  $\mathbf{R}_{\text{tip}}$ . The window function, which is a zero-temperature approximation to the product of Fermi-Dirac functions in Eq. (1), specifies that only sample states with energies between  $E_F$  and  $E_F - eV$  contribute to the tunneling current. To compute the STM images, we assume that the energy-selected sample charge density, Eq. (3), evaluated at constant tip height of  $\approx 4.5$  Å, gives a good approximation to the image taken under constant current conditions.

Our computed STM images of empty states (+2.0-V bias) and filled states (−1.8-V sample bias) are shown in Figs. 6(a) and 6(b).<sup>41</sup> They agree well with the experimental images shown in Figs. 5(a) and 5(b). In particular, the empty-state contours [Fig. 6(a)] show a trimer structure with lobes oriented along the  $\langle 110 \rangle$  direction, the direction of the bond between the Co and the Si capping adatoms. The total density of states (see Fig. 4) in the region  $\approx 1$  eV above the Fermi level contains contributions from the  $s$  and  $p_z$  orbitals on the Si capping adatoms, the  $s$  orbitals of the bridging adatoms, and the  $p$  and  $d$  orbitals of the Co atoms. Tunneling into empty states proceeds primarily through the empty states on the Si capping adatoms, both because the capping Si adatoms

are highest above the surface (0.41 Å above the bridging Si adatoms and 1.48 Å above the Co atoms), and because the  $p_z$  orbitals are directed up from the surface toward the STM tip. Positive (sample) bias tunneling yields images of the Si capping adatoms.

In Fig. 6(b), the filled states’ contours show a single lobe in the surface unit cell, corresponding to the Co atoms’ positions. Tunneling from filled states is dominated by the  $d$  states on the Co atom, even though the Si capping atoms are 1.5 Å closer to the tip, because of the much larger density of states associated with the rather flat Co  $d$  bands below  $E_F$ .

Thus the theoretical STM images are similar to the STM images that led to the ring-cluster model—lending further support to the model.

#### D. Magnetic moments

Our spin-unrestricted calculations show that the ring-cluster model of the  $\sqrt{7} \times \sqrt{7}$  surface has essentially no net magnetization. However, the electronic system itself is slightly spin polarized: within a sphere of radius 1.11 Å centered on a Co atom, the computed net magnetic moment is 0.0655 Bohr magnetons. Electrons in the regions surrounding the Co are spin polarized in the opposite direction to the spin of the Co atom.

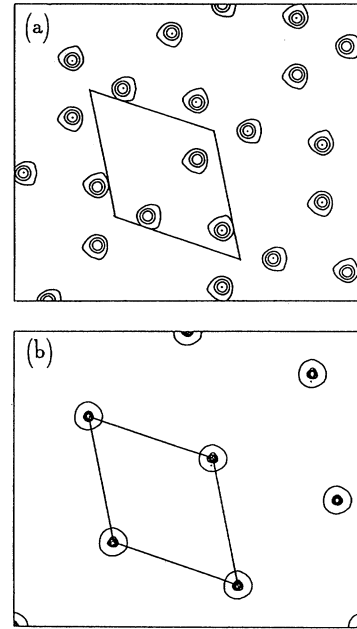


FIG. 6. Calculated STM images of the ring-cluster model, using the approximation that the image is an energy-selected charge density (of occupied or empty states) at a fixed tip height of 4.5 Å above the surface plane. We show only contours of constant partial charge density within 70% of the maximal partial charge densities. (a) For a positive sample bias of 2.0 V, showing capping-Si sites; and (b) for a sample bias of −1.8 V (tunneling of electrons from the sample to the tip), showing Co sites.

### E. Bistability and solitons

The ring-cluster structure is mechanically bistable, because the roles of capping and bridging adatoms can be interchanged, leaving an energetically equivalent configuration in each unit cell. Of course, the nuclei themselves need not actually move between sites, only the valence electrons need move appreciably, with the atoms themselves moving only slightly to accommodate the new bond lengths. Thus the system has a degenerate ground state and should exhibit solitons. This raises the questions of whether it can switch between equivalent states as a result of thermal excitation: excitation of a "kink."

We make a crude attempt to address this problem by computing the total energy of an assumed configuration intermediate between the two degenerate ground-state configurations. This intermediate configuration has  $C_6$  symmetry<sup>11</sup> and could conceivably (but does not) break up into three  $\pi$ -bonded pairs of adatoms. We put the Co atom at its ground-state position (in the ring cluster), and require all six Si adatoms to lie 2.607 Å away (at sites intermediate between the bridging and capping positions in the ground state). The total energy for this configuration is 1.2 eV per  $\sqrt{7} \times \sqrt{7}$  surface unit cell higher than the ground-state energy. This is too large for switching between equivalent states of the *extended*  $\sqrt{7} \times \sqrt{7}$  structure to occur at room temperature.

The situation will be different for an *isolated* ring cluster, if a significant fraction of that 1.2 eV activation energy for the close-packed structure comes from cluster-cluster interactions that were necessarily included in the calculations due to the assumed periodicity. The relatively high (experimental) disordering temperature of 700 °C suggests that these interactions are significant. Then the isolated structures would have a considerably lower activation energy for switching. In addition, relaxed steric constraints on the isolated cluster could also result in lower-energy pathways for switching, perhaps through concerted<sup>42</sup> or collective motion of the atoms. If, for example, the isolated character of a cluster were to allow switching via the thermal motion of *two* Si adatoms (instead of  $6N$  for the close-packed surface) which would then initiate the motion of the remaining four adatoms of the cluster, then the relevant activation energy would be approximately  $E_S = 0.4$  eV per adatom pair. We could crudely estimate a switching rate for such a process as  $\tau^{-1} \approx \nu \exp(-E_S/k_B T)$ , where  $\nu \approx 10^{13} \text{ s}^{-1}$  is a typical phonon frequency, and  $E_S \approx 0.4$  eV. Then we have

$\tau \geq 10^{-6} \text{ s}$ . This is much faster than the time required to scan over a given ring cluster with the STM ( $\approx 20 \text{ s}$ ), so experimental images would correspond to a superposition of the two orientations. The ringlike appearance of isolated clusters in Figs. 5(a) and 5(c) is suggestive of this interpretation. This speculation could be confirmed by cooling the sample, as has been done to demonstrate analogous dimer switching on the Si(100) surface.<sup>43</sup>

### V. CONCLUSIONS

Our calculations thoroughly support the ring-cluster model of one-seventh monolayer coverage of Co on the Si(111) surface. The model features bond lengths and bond angles that correspond to a local minimum of the total energy; it produces STM images in agreement with the observations; and its degenerate ground state is theoretically bistable. *A close-packed array of ring clusters* is not expected to exhibit bistability and solitons at temperatures near 300 K. However, isolated ring clusters might. It would be interesting if photoemission measurements were to confirm the model's calculated electronic structure of Fig. 4.

The remarkable stability of the ring-cluster structure and the similarity of its bonding to that of bulk  $\text{CoSi}_2$  suggest that it may play an important role in silicide reactions, particularly at high temperatures. Surface transport of metal atoms at high temperatures may occur via motion of these clusters.<sup>8</sup> The ring clusters may be precursors to the formation of  $\text{CoSi}_2$ , at least during deposition at high temperatures, when metal atoms occupy a Si-rich environment on the surface. Likewise, they may represent an intermediate step in the dissolution of metal atoms from a silicide overlayer into the bulk substrate. Further studies of the ring-cluster structure, particularly at high temperatures, should prove to be very illuminating.

### ACKNOWLEDGMENTS

We are grateful for the generous support of the U.S. Office of Naval Research, the U.S. Air Force Office of Scientific Research, and the National Science Foundation (Grant Nos. N00014-92-J-1425, AFOSR-91-0418, and DMR89-21124). We also acknowledge useful discussions with J. E. Demuth, R. M. Tromp, and M. Copel and support from the IBM T. J. Watson Research Center during the sabbatical leave of P.A.B.

<sup>1</sup>M. A. Nicolet and S. S. Lau, in *VLSI Microelectronic Science*, edited by N. G. Einspruch and G. B. Larrabee (Academic, New York, 1983), p. 330.

<sup>2</sup>K. N. Tu and J. W. Mayer, in *Thin Films—Interdiffusion and Reactions*, edited by J. M. Poate, K. N. Tu, and J. W. Mayer (Wiley, New York, 1978), p. 359.

<sup>3</sup>See, for example, P. J. van den Hoek, W. Ravenek, and E. J. Bacrends, *Phys. Rev. Lett.* **60**, 1743 (1988), and references therein.

<sup>4</sup>L. J. Chen, H. C. Cheng, and W. T. Lin, in *Thin Films—Interfaces and Phenomena*, edited by R. J. Nemanich, P. S.

Ho, and S. S. Lau, *MRS Symposia Proceedings No. 54* (Materials Research Society, Pittsburgh, 1986), p. 245.

<sup>5</sup>D. D. Chambliss and T. N. Rhodin, *Phys. Rev. B* **42**, 1674 (1990).

<sup>6</sup>R. J. Wilson and S. J. Chiang, *Phys. Rev. Lett.* **58**, 2575 (1987).

<sup>7</sup>K. Akiyama, K. Takayanagi, and Y. Tanishiro, *Surf. Sci.* **205**, 177 (1988).

<sup>8</sup>P. A. Bennett, M. Copel, D. Cahill, J. Falta, and R. M. Tromp, *Phys. Rev. Lett.* **69**, 1224 (1992).

<sup>9</sup>The basis vectors are  $\mathbf{a}_1 = (\frac{5}{2}, -\sqrt{\frac{3}{2}})(a_L/\sqrt{2})$  and  $\mathbf{a}_2 = (-\frac{1}{2}, 3\sqrt{\frac{3}{2}})(a_L/\sqrt{2})$ . The coordinates of the Co atom

- are  $(0,0,h)$ , where we have  $h = 0.1206a_L/\sqrt{2}$ . The bridging Si adatoms are at  $(-0.5346, 0, 0.3980)a_L/\sqrt{2}$ ,  $(0.2673, 0.4630, 0.3980)a_L/\sqrt{2}$ , and  $(0.2673, 0.4630, 0.3980)a_L/\sqrt{2}$ . The capping Si adatoms are at the positions  $(0.6532, 0, 0.5050)a_L/\sqrt{2}$ ,  $(-0.3268, -0.5660, 0.5050)a_L/\sqrt{2}$ , and  $(-0.3268, 0.5660, 0.5050)a_L/\sqrt{2}$ . The first-layer Si atoms are at  $(1,0,0)a_L/\sqrt{2}$ ,  $(-\frac{1}{2}, \sqrt{\frac{3}{2}}, 0)a_L/\sqrt{2}$ ,  $(-\frac{1}{2}, -\sqrt{\frac{3}{2}}, 0)a_L/\sqrt{2}$ ,  $(-1,0,0)a_L/\sqrt{2}$ ,  $(\frac{1}{2}, -\sqrt{\frac{3}{2}}, 0)a_L/\sqrt{2}$ , and  $(\frac{1}{2}, \sqrt{\frac{3}{2}}, 0)a_L/\sqrt{2}$ . Here we have  $a_L = 5.431$  Å.
- <sup>10</sup>CoSi<sub>2</sub> has the CaF<sub>2</sub> structure with a Co-Si bond length of 2.324 Å.
- <sup>11</sup>We use the standard chemical notation; see, for example, M. Tinkham, *Group Theory and Quantum Mechanics* (McGraw-Hill, New York, 1964).
- <sup>12</sup>L. F. Matthiess and D. R. Hamann, Phys. Rev. Lett. **54**, 2517 (1985).
- <sup>13</sup>*Table of Periodic Properties of the Elements* (Sargent-Welch, Skokie, IL, 1979).
- <sup>14</sup>W. Kohn and L. J. Sham, Phys. Rev. **140**, 1133 (1965).
- <sup>15</sup>*CRC Handbook of Chemistry and Physics*, 72nd ed., edited by David R. Lide (Chemical Rubber, Boca Raton, 1991).
- <sup>16</sup>Even with surface reconstruction, the Si-Si bond-length changes are small, typically less than 2%. See D. J. Chadi, Phys. Rev. Lett. **43**, 43 (1979).
- <sup>17</sup>M.-H. Tsai, J. D. Dow, R. V. Kasowski, A. Wall, and A. Franciosi, Solid State Commun. **69**, 1131 (1989); R. V. Kasowski, M.-H. Tsai, and J. D. Dow, Phys. Rev. B **41**, 8949 (1990).
- <sup>18</sup>The spin-unrestricted pseudofunction method is an extension of the paramagnetic pseudofunction method of R. V. Kasowski, M.-H. Tsai, T. N. Rhodin, and D. D. Chambliss, Phys. Rev. B **34**, 2656 (1986). In this method, the starting potential for self-consistent iterations is obtained by overlapping spin-unrestricted atomic potentials and charge densities, which are calculated from a spin-unrestricted self-consistent atomic program.
- <sup>19</sup>U. von Barth and L. Hedin, J. Phys. C **5**, 1629 (1972).
- <sup>20</sup>A. Franciosi, A. Wall, Y. Gao, J. H. Weaver, M.-H. Tsai, J. D. Dow, R. V. Kasowski, R. Reifenberger, and F. Pool, Phys. Rev. B **40**, 12009 (1989).
- <sup>21</sup>A. Wall, A. Franciosi, Y. Gao, J. H. Weaver, M.-H. Tsai, J. D. Dow, and R. V. Kasowski, J. Vac. Sci. Technol. A **7**, 656 (1989).
- <sup>22</sup>R. V. Kasowski, M.-H. Tsai, J. D. Dow, and M. T. Czyzyk, Physica C **162**, 1349 (1989).
- <sup>23</sup>R. V. Kasowski, J. Am. Ceram. Soc. **73**, 3170 (1990).
- <sup>24</sup>R. H. French, R. V. Kasowski, F. S. Ohuchi, D. J. Jones, H. Song, and R. L. Coble, J. Am. Ceram. Soc. **73**, 3195 (1990).
- <sup>25</sup>R. V. Kasowski, P. Soukiassin, and G. Collin, Solid State Commun. **77**, 135 (1991).
- <sup>26</sup>M.-H. Tsai, J. D. Dow, and R. V. Kasowski, Phys. Rev. B **38**, 2176 (1988).
- <sup>27</sup>M.-H. Tsai, O. F. Sankey, and J. D. Dow, Phys. Rev. B **46**, 10464 (1992).
- <sup>28</sup>S. L. Cunningham, Phys. Rev. B **10**, 4988 (1974).
- <sup>29</sup>This two-dimensional special point is  $\mathbf{k}_{\parallel} = 0.38(\frac{1}{7}, \frac{3}{14}\sqrt{3})(2\sqrt{2}\pi/a_L)$ , where  $a_L$  is the lattice constant.
- <sup>30</sup>C. K. Shih, R. M. Feenstra, and G. V. Chandrashekhar, Phys. Rev. B **43**, 7913 (1991).
- <sup>31</sup>J. P. Pelz, Phys. Rev. B **43**, 6746 (1991).
- <sup>32</sup>L. Pauling and A. M. Soldate, Acta Crystallogr. **1**, 212 (1948).
- <sup>33</sup>J. Vrijmoeth, A. G. Shins, and J. F. van der Veen, Phys. Rev. B **40**, 3121 (1989).
- <sup>34</sup>See, for example, D. D. Chambliss, T. N. Rhodin, and J. E. Rowe, Phys. Rev. B **45**, 1193 (1992), and references therein; also Ref. 26 and references therein.
- <sup>35</sup>J. Tersoff and D. R. Hamann, Phys. Rev. Lett. **50**, 2002 (1983).
- <sup>36</sup>J. V. Florio and W. D. Robertson, Surf. Sci. **24**, 173 (1971).
- <sup>37</sup>R. J. Hamers, R. M. Tromp, and J. E. Demuth, Phys. Rev. B **34**, 5343 (1986).
- <sup>38</sup>J. Gryko and R. E. Allen, J. Ultramicroscopy **42-44**, 793 (1992).
- <sup>39</sup>J. Bardeen, Phys. Rev. Lett. **6**, 57 (1961).
- <sup>40</sup>J. Tersoff and D. R. Hamann, Phys. Rev. Lett. **50**, 2002 (1983).
- <sup>41</sup>The Fermi energy in our model surface lies at the top of the filled states, but, on a real surface, the Fermi level is pinned at approximately midgap (J. Bardeen, Phys. Rev. **71**, 717 (1947); J. D. Dow, R. E. Allen, and O. F. Sankey, *Intrinsic and Extrinsic Surface Electronic States of Semiconductors, Chemistry and Physics of Solid Surfaces V*, edited by R. Vanselow and R. Howe, Springer Series in Chemical Physics Vol. 35 (Springer-Verlag, Berlin, 1984), pp. 483–500; J. D. Dow, O. F. Sankey, and R. E. Allen, *Chemical Trends of Schottky Barriers*, Materials Science Forum Vol. 4 (Trans Tech, Switzerland, 1985), pp. 39–50; R. E. Allen, O. F. Sankey, and J. D. Dow, in *Proceedings of the International Conference on the Formation of Semiconductor Interfaces, Marseilles, 1985*, edited by G. Le Lay [Surf. Sci. **168**, 376 (1986)]). This changes the bias conditions of our simulations from  $-1.8$  and  $+2.0$  V to about  $-1.3$  and  $+2.5$  eV. The essential features of the images will be unchanged, however, since the single-lobe Co structure is characteristic of negative bias, and the trilobe Si capping-adatom structure is characteristic of positive bias.
- <sup>42</sup>K. C. Pandey and E. Kaxiras, Phys. Rev. Lett. **66**, 915 (1991).
- <sup>43</sup>R. A. Wolkov, Phys. Rev. Lett. **68**, 2636 (1992).

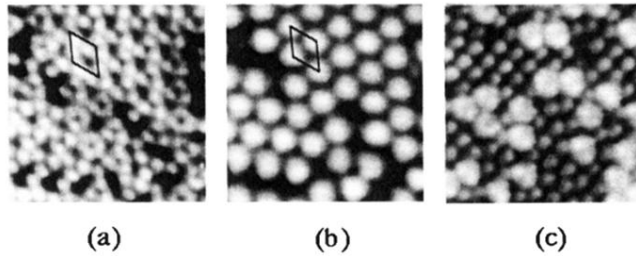


FIG. 5. Experimental STM images showing various arrangements of ring-cluster structures. (a) The empty-state image (bias of +2.0 V) of the  $\sqrt{7} \times \sqrt{7}$  structure with a single surface unit cell outlined. For close-packed structures, clearly defined trimer lobes point in the directions of the  $\langle 110 \rangle$  azimuths, while isolated clusters take on a more closely sixfold-symmetric appearance. (b) The filled-state image (bias of -1.8 V) of the matching area showing a single lobe at the center of the trimers. (c) The empty-state image (+2.2 V) of the (cobalt) “impurity-stabilized  $1 \times 1$ ” surface produced by heating to 1250°C. It is a lattice gas of ring clusters. Again, note the apparent loss of threefold symmetry for individual, isolated ring clusters.